



Monsoon variability and chemical weathering during the late Pleistocene in the Goriganga basin, higher central Himalaya, India

Steven P. Beukema^{a,b,*}, R.V. Krishnamurthy^a, N. Juyal^c, N. Basavaiah^d, A.K. Singhvi^c

^a Department of Geosciences, Western Michigan University, Kalamazoo, MI, USA

^b Michigan Department of Environmental Quality, Kalamazoo, MI, USA

^c Physical Research Laboratory, Ahmedabad 380 009, India

^d Indian Institute of Geomagnetism, Colaba, Mumbai 400 005, India

ARTICLE INFO

Article history:

Received 25 February 2008

Available online 28 January 2011

Keywords:

Himalaya
Stable isotopes
Lacustrine sediments
Younger Dryas
Paleoclimate
Hardwater effect
Luminescence dating
Late Pleistocene
Monsoon
Chemical weathering

ABSTRACT

Stable isotope analysis along with radiocarbon and luminescence dating of late Pleistocene lacustrine deposits at Burfu in the higher central Himalaya are used to interpret hydrologic changes in the lake basin. From 15.5 ka to ~14.5 ka the Burfu lake was largely fed by melting glaciers. A warming event at 14.5 ka suggests an enhanced monsoon and increased carbonate weathering. From ~13.5 ka to ~12.5 ka the isotopic data suggest large-amplitude climate variability. Following this, the isotope data suggest a short-lived, abrupt cooling event, comprising a ~300-yr intense cool period followed by a ~500-yr interval of moderate climate. A shift in isotope values at ~11.3 ka may signify a strengthening monsoon in this region. The inferred climatic excursions appear to be correlative, at least qualitatively, with global climatic events, and perhaps the Burfu lake sequence provides regional evidence of globally recorded excursions. This study also suggests a potential use of radiocarbon ages in specific environments as a paleoenvironmental proxy.

© 2011 Published by Elsevier Inc. on behalf of University of Washington.

Introduction

The Himalayas contains the third largest concentration of snow and ice cover in the world. The Ganges River, one of the major rivers in north India, originates from glacial meltwater streams in the higher central Himalaya, and precipitation associated with the southwest Indian summer monsoon (ISM) also contributes to the Ganges River. The dynamics of glaciers in north India and the strength of the ISM are forced by changes in insolation and albedo (Prell and Kutzbach, 1992; Bush, 2000). An understanding of regional variations in the Himalayan glaciers and the ISM in response to global climate change is critical to evaluate and predict the hydrologic balance of major rivers in this part of the world.

Extensive exposures of late Pleistocene lacustrine deposits are present in the tributaries of the higher central Himalaya, north India. One such lacustrine succession near the village of Burfu in the Goriganga basin was analyzed for stable isotopes, radiocarbon and optically-stimulated luminescence (OSL) dating. The data are evaluated to answer three questions: 1) what late Pleistocene climate changes are recorded in this region and if the inferred climate excursions in the Himalaya follow a pattern similar to global climate

changes; 2) do changes in monsoon affected the magnitude of chemical weathering of carbonates; and 3) do the discordance between radiocarbon and luminescence ages arises due to climatic reasons?

Geology and geomorphology

Lacustrine deposits near the village of Burfu are located in the Goriganga basin of the central Himalaya (30°21'40.3"N, 80°10'57.3"E). This succession is exposed along the Kharkhan Khotla stream, a tributary to the Goriganga, which originates from a glacier at the head of the Kharkhan Khotla stream (Fig. 1). Pant et al. (2006) identified three glacial advances (Stage-I to III) in the Goriganga valley. The Stage-I moraine is the oldest and longest that terminates near Rilkot (~3100 m.a.s.l.). Based on geomorphology and stratigraphic position, it was assigned a pre-last glacial maximum (LGM) age, probably equivalent to the Bhagirathi glacial stage (~63 ka–11 ka) of Sharma and Owen (1996) and Barnard et al. (2004a). The Stage-II moraine terminates near the present lake deposits (~3300 m.a.s.l.). Lake sediments immediately overlying the Stage-II ground moraine were luminescence dated to 16.5 ka (Pant et al., 2006), hence it was assigned an LGM age. The Stage-III moraine was suggested to correspond to the Little Ice Age following the study of Barnard et al. (2004b) at Milam glacier.

* Corresponding author. Michigan Department of Environmental Quality, Remediation Division, 7953 Adobe Road, Kalamazoo, Michigan 49009, USA. Fax: +1 269 567 9440.

E-mail address: beukemas@michigan.gov (S.P. Beukema).

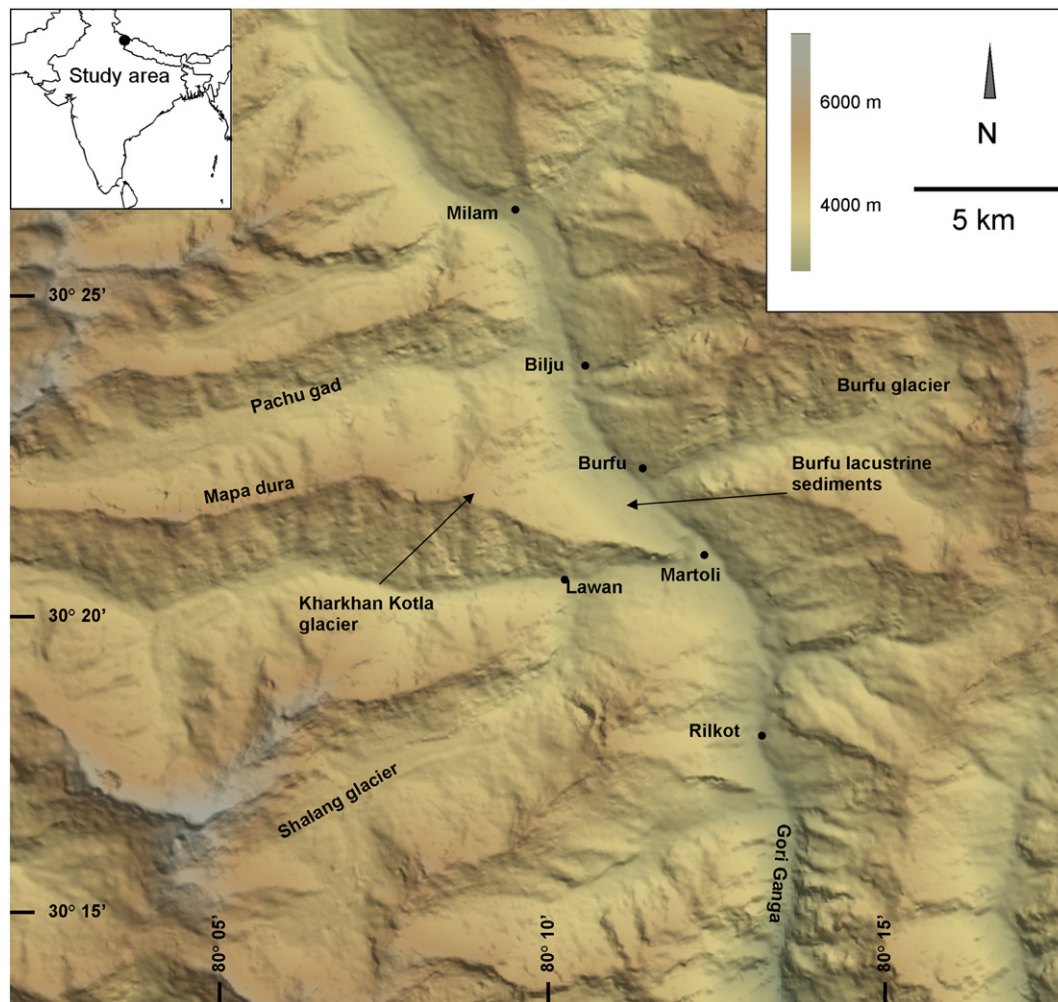


Figure 1. DEM showing the location of the study area. Local villages are represented by black dots.

The clast lithology of the moraines beneath the lake succession is dominated by boulders of phyllite with subordinate calc-silicates and slate. Calc-silicate rocks occur around 10 km upstream in the Martoli valley (Shalang glacier). Field evidence suggests that a moraine was deposited during the Stage-II glaciation by the glacier at the head of the Kharkhan Khotla stream. During the retreat the glacial stream was impounded by the moraine, and a ~23-m-thick lacustrine succession was deposited.

The NW–SE trending Trans-Himadri Fault (THF) runs parallel to the Goriganga until Martoli. North of Martoli the THF trends WNW parallel to the Kalchu and Mapa Dhura (Dhura=ridge). The glacier that feeds the Kharkhan Khotla stream lies on this ridge (Fig. 1). The THF defines the tectonic boundary between the southern central crystalline rocks (quartzite, quartz schist, gneisses and migmatite) and the Martoli and Ralam formation in the north. The catchment lithology near the Burfu lacustrine sediments is dominated by Tethyan sedimentary rocks comprising phyllite, quartzite, calc-silicates, black shale, dolomitic limestone, and brown marl (Sinha, 1981).

Stratigraphy of the lake

The late Pleistocene lacustrine succession at Burfu overlies a ground moraine at 3300 m.a.s.l. (Fig. 2). The glacier at the head of the Kharkhan Khotla stream is presently at an elevation of 4500 m.a.s.l. and is located on the Kalchu and Mapa Dhura ridge (Fig. 1).

The lacustrine succession is divided into three sedimentary units (Fig. 3). The lowermost Unit-I (~7.2 m) overlies the ground moraine

and is dominated by well-sorted medium to fine sand with occasional clay laminae. This is overlain by Unit-II (~6.2 m), comprising clay-rich varves with mm- to cm-thick sand intercalations (Fig. 4). At places dropstones are embedded in the varve layers. The uppermost Unit-III (~10 m) comprises thicker internally laminated clay horizons (<120 cm thick). The clay horizons are generally separated by medium to fine sand layers (<30 cm) and the succession terminates with a ~2-m-thick debris-flow deposit.

Chronology

Seven samples for OSL dating were collected from freshly exposed trenches using specially designed aluminum pipes (Chandel et al., 2006). The basic principles of luminescence dating are discussed in Singhvi et al. (2001, 2011). The dating of sediments from glacial environments has been recently reviewed by Fuchs and Owen (2008). Samples were treated with 10% HCl and 30% H₂O₂ to remove the carbonate and organic carbon, respectively. This was followed by the removal of mica by placing the sample on a charged transparency sheet. The samples were then dry-sieved to obtain grain sizes in the ranges of 210–150 μm and 150–105 μm. Quartz and feldspar minerals were separated using Na-polytungstate ($\rho = 2.58 \text{ g/cm}^3$). The quartz-rich fraction was further etched for 80 min in 40% HF followed by a reaction with 12 N HCl for 30 min. The etched grains were mounted as a monolayer on stainless steel discs using Silkospray™ and the purity of these grains was checked by infrared-stimulated luminescence. The samples were generally whitish with few heavy grains, but the shape



Figure 2. Photograph of Burfu lacustrine sediments. Dark sediment at the base of the exposure is a ground moraine. Thickness of lacustrine section is approximately 23 m.

of the shine-down curve indicated that these samples originated from quartz. The samples were stimulated using a blue-green light stimulation source from a Riso TA-DA-15 reader and the detection optics comprised 2×U-340 and BG-39 filters. Beta irradiation was made using a 25 mCi ⁹⁰Sr/⁹⁰Y source. The dose-rate estimates relied

on thick source ZnS(Ag) alpha counting for elemental concentrations of uranium and thorium, whereas the potassium concentration was estimated using gamma ray spectrometry (hyper-pure germanium detector). A constant cosmic ray dose was used because in any accreting sedimentary system, the cosmic ray flux changes with

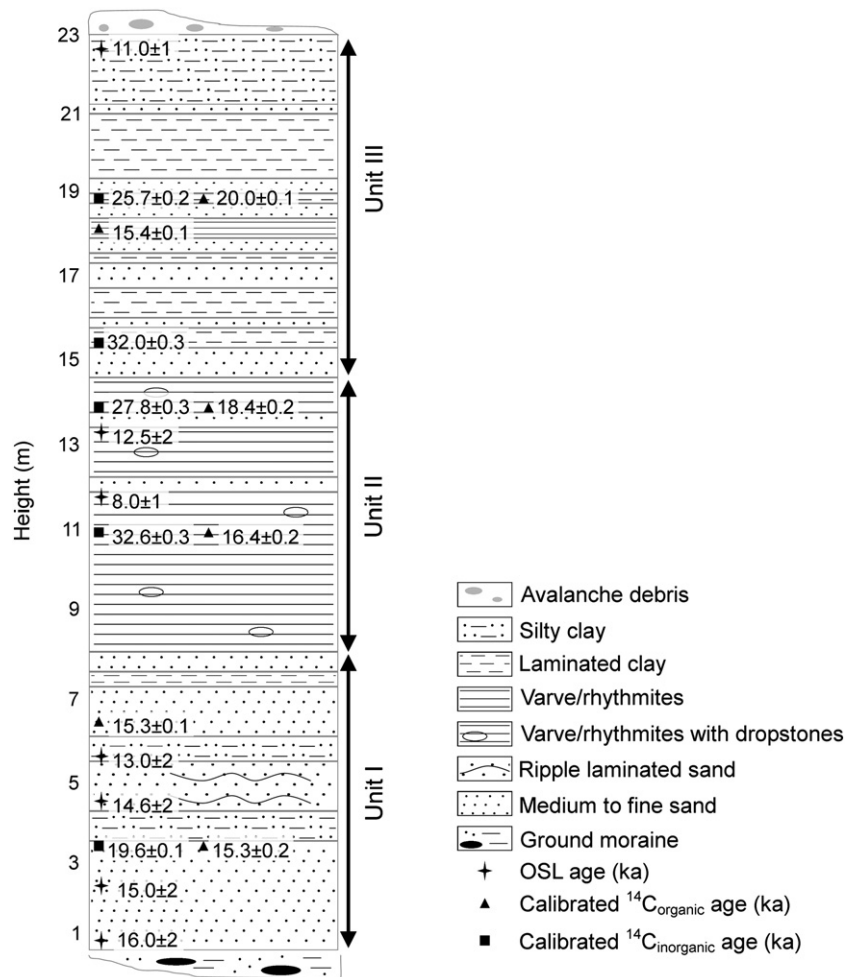


Figure 3. Burfu lake succession stratigraphy with OSL ages, calibrated ¹⁴C ages from the carbonate and organic fraction. Modified after Pant et al. (2006).

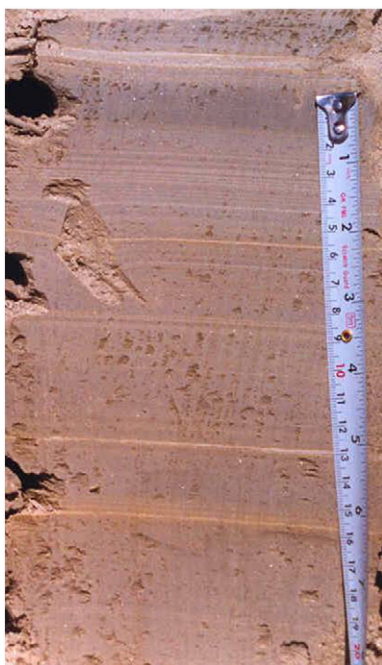


Figure 4. Close-up photograph of Burfu lacustrine sediments showing mm-thick varves and laminae.

increasing overburden. An accurate calculation of cosmic ray dose would then require an estimate of the rate of increase of overburden. This would need an estimate of the duration and the rate of burial (i.e., age and sedimentation rate). As these are the quantities to be determined, the estimation of the time dependence of the cosmic ray dose rate becomes dependent on the model for sedimentation. Given that the cosmic ray constitutes <5% of the total signal, it implies a near-identical error of a few percent on account of such uncertainties. Such small systematic errors would not upset any of the conclusions from the present study (Juyal et al., 2006). For the cosmic ray exposure at an elevation of ~3000 m, the dose rate at the surface is computed to be ~350 $\mu\text{Gy/yr}$ and it reduces to 30 $\mu\text{Gy/yr}$ at a depth of 20 m. Given an exponential decrease of the dose rate, we used a constant value of $190 \pm 30 \mu\text{Gy/yr}$ as a reasonable approximation.

The samples were analyzed using the single aliquot regeneration (SAR) protocol of Murray and Wintle (2000). The aliquots were preheated to 240°C for 10 s and the cut heat was 200°C. Typically about 50–60 discs were measured and of these around 20–40 satisfied the criterion of a recycling ratio of 0.90–1.10. The paleodose for age calculations was based on a weighted mean of values in the region defined by the minimum value and the minimum value + ($2 \times \text{error}$) (Juyal et al., 2006). Typically about 5–10 paleodoses belonged to this realm. Table 1 provides the details of radioactivity assays, dose rate and SAR ages (both minimum and mean). Stratigraphic locations of OSL ages are shown in Figure 3.

Table 1
BGSL (SAR) ages on Burfu lake succession.

| Sample No. (ka) | U (ppm) | Th (ppm) | ^{40}K (%) | Dose Rate (Gy/ka) | De (Gy) | Age (ka) |
|-----------------|-----------------|----------------|---------------------|-------------------|------------|--------------|
| BLTL-13 | 3.82 ± 0.06 | 19.3 ± 0.3 | 2.6 ± 0.03 | 3.9 ± 0.5 | 44 ± 1 | 11.0 ± 1 |
| BLTL-10 | 3.14 ± 0.05 | 16.1 ± 0.3 | 1.81 ± 0.02 | 3.1 ± 0.4 | 38 ± 1 | 12.5 ± 2 |
| BLTL-9 | 3.24 ± 0.05 | 16.6 ± 0.3 | 2.11 ± 0.02 | 3.4 ± 0.4 | 28 ± 1 | 8.0 ± 1 |
| BLTL-6 | 3.01 ± 0.04 | 17.0 ± 0.2 | 1.41 ± 0.01 | 2.8 ± 0.4 | 37 ± 1 | 13.0 ± 2 |
| BLTL-5 | 3.28 ± 0.05 | 18.5 ± 0.3 | 2.47 ± 0.02 | 3.7 ± 0.5 | 54 ± 2 | 14.6 ± 2 |
| BLTL-2 | 3.15 ± 0.05 | 20.5 ± 0.3 | 1.64 ± 0.01 | 3.2 ± 0.4 | 48 ± 2 | 15.0 ± 2 |
| BLTL-1 | 3.4 ± 0.05 | 21.1 ± 0.3 | 1.66 ± 0.02 | 3.3 ± 0.4 | 53 ± 1 | 16.0 ± 2 |

Cosmic ray dose assumed $190 \pm 40 \mu\text{Gy/a}$.
Water content assumed $20 \pm 10\%$.

An aspect that merits consideration is the extent of bleaching at the time of deposition given that fluvial transport could result in incomplete bleaching due to turbid conditions. However, higher ultraviolet radiation at sampling altitudes with high efficiency of bleaching of OSL, clear, dust-free sky conditions, and still and clean water conditions in the environment of such lakes implies a reasonable assumption that the samples were bleached at the time of deposition. This is also borne out by the fact that the average deposition rate is ~few cm/yr and earlier studies by Kronborg (1983) also indicated that samples underwater can be bleached. The overall stratigraphic consistency of ages indicates that adequate bleaching occurred to give reliable ages using a minimum age criterion. As a caveat, we suggest that though we consider the ages as realistic, in a worst-case scenario the OSL ages would represent an upper limit for the ages. We refer to an excellent overview by Fuchs and Owen (2008) on the theory, methodology and reliability of OSL ages in glacial environments.

In addition to the OSL ages, six AMS ^{14}C ages from bulk organic carbon samples and five authigenic carbonate samples were obtained (Table 2). Radiocarbon analysis was performed at the University of Arizona AMS Laboratory. Radiocarbon dates were converted to calendar years before present using the Fairbanks calibration curve (Fairbanks et al., 2005). The radiocarbon dates were not used in the age model due to the 'hardwater effect' in this region as is evident from the random behavior of ages. This has been discussed in detail by Fontes et al. (1996) and by Juyal et al. (2004) in the context of the Himalaya. We infer that samples with a much older radiocarbon age compared to OSL age contain dead carbon and we interpret a large difference in age as enhanced chemical weathering of carbonates in the catchment area.

An age model was calculated by performing a weighted linear least squares regression on six OSL ages (Fig. 5). Despite larger error limits, OSL ages were used for the present study, and as a best case scenario a constant accumulation rate was used. Though this may not be the most accurate description of the sedimentation rate, a glance at Figure 5 indicates that due to the narrow age span (16–11 ka) there cannot be much variability between any sedimentation model that can be applied to these ages compared to the constant sedimentation rate. We therefore do not consider that any of the interpretations presented here would change appreciably with another age model.

Stable isotope analysis

For stable isotope analysis, the sampling interval was 10 cm, corresponding approximately to a sample every 20 yr. The samples were divided into two fractions. The first fraction was used for the isotopic analysis of organic carbon and for C/N ratios, and the second fraction was used for isotopic analysis of carbon and oxygen from the carbonate fraction. The samples for the organic fraction and the carbonate fraction were prepared using procedures outlined by Krishnamurthy et al. (1997, 1999). Isotopic analysis was carried out using a Micromass Optima dual inlet isotope ratio mass spectrometer.

Table 2
Radiocarbon ages on Burfu lake succession.

| Sample No. | Height (m above bottom) | Age (¹⁴ C yr BP) | Material | Calibrated age (yr BP) |
|------------|-------------------------|------------------------------|-----------|------------------------|
| AA64524 | 19.05 | 21,440 ± 150 | Inorganic | 25,741 ± 243 |
| AA64523 | 15.35 | 26,720 ± 260 | Inorganic | 32,007 ± 317 |
| AA64522 | 13.85 | 23,180 ± 200 | Inorganic | 27,811 ± 264 |
| AA64521 | 11.2 | 27,300 ± 280 | Inorganic | 32,625 ± 335 |
| AA64519 | 3.55 | 16,524 ± 87 | Inorganic | 19,638 ± 107 |
| AA64518 | 19.05 | 16,840 ± 100 | Organic | 20,005 ± 138 |
| AA64517 | 18.25 | 13,257 ± 75 | Organic | 15,437 ± 135 |
| AA64515 | 13.85 | 15,160 ± 130 | Organic | 18,366 ± 213 |
| AA64514 | 11.2 | 14,030 ± 150 | Organic | 16,388 ± 244 |
| AA64513 | 6.6 | 13,173 ± 72 | Organic | 15,341 ± 131 |
| AA64512 | 3.55 | 13,170 ± 120 | Organic | 15,338 ± 171 |

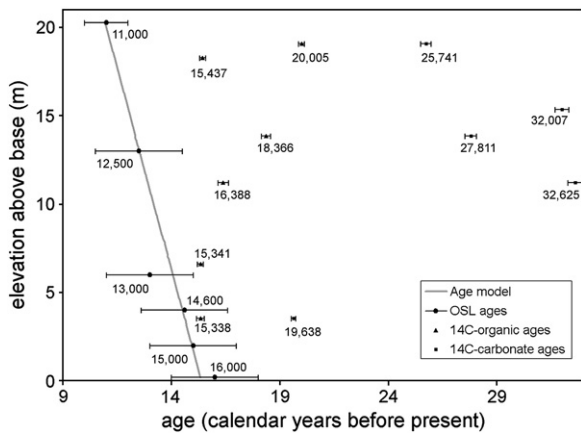


Figure 5. Age model of the Burfu section.

Analytical precision for $\delta^{13}\text{C}$ was 0.1‰ and for $\delta^{18}\text{O}$ was 0.2‰. All isotopic results are reported in the standard permil (‰) notation with respect to VPDB.

The stable isotope analyses are presented in Figure 6. In order to eliminate random variations due to the coarseness of sampling (1 sample per approximately 20 yr) the data were smoothed with a 5-point running average. The $\delta^{18}\text{O}$ values show significant variability with an overall trend toward higher values from -15‰ (at the base) to -10‰ at the top. An increase of 2‰ until 4 m above the base of the section is followed by a decrease by $\sim 1.5\text{‰}$, after which there is a steady trend toward higher oxygen isotope values. From 9 m above the base to the top of the section, a series of rapid high-amplitude fluctuations in $\delta^{18}\text{O}$ values occurs, including spikes in the positive direction at 11 m and 14 m. Both of these spikes are followed by sharp, negative excursions. The final abrupt shift to positive values occurs at 20 m.

$\delta^{13}\text{C}_{\text{carbonate}}$ values also show an overall increasing trend from -3.5‰ to -1‰ . The largest shift in carbon isotope values occurs at 4.5 m. From 4.5 m to 9 m there is a gradual trend toward more positive

values, and from 10 m to 15 m there are several high-amplitude changes. At 16 m there is a large shift to negative values, followed by a large shift in the positive direction. A final shift in the positive direction occurs at 20 m.

The percentage of carbonate remains relatively constant throughout the section, with a higher amount of carbonate occurring until ~ 7 m above the base. The percentage of organic carbon is relatively constant at approximately 0.2% throughout the section. Values of $\delta^{13}\text{C}_{\text{organic}}$ are also relatively constant throughout the section, with values averaging -23‰ . C/N ratios throughout the lake section are <5 with the exception of the interval between 4 m to 6 m, where C/N ratios reach as high as 15.

Discussion

It is difficult to link the oxygen isotope values of lacustrine sediments to a single climatic variable, as all of the variables that control the isotopic values are intricately interconnected (Leng and Marshall, 2004). For example, a change in temperature is likely to result in a concomitant change in monsoon strength and therefore hydrologic changes in the basin. As the sources of water in this region exhibit widely varying stable isotopic signatures (Ghosh and Bhattacharya, 2003), it is likely that the $\delta^{18}\text{O}$ signature of the source water determines the $\delta^{18}\text{O}$ values of the carbonates precipitated in the lake. At high elevations in the Himalaya, waters in river and lacustrine environments are from isotopically depleted glacial meltwater (Owen and Sharma, 1998). For example, regional glacial meltwater (near Goting, ~ 100 km NW of Burfu) has an average $\delta^{18}\text{O}$ value of -20.3‰ , whereas river water and snowmelt in the area have higher $\delta^{18}\text{O}$ values of -13.0‰ and -13.5‰ , respectively (Ghosh and Bhattacharya, 2003). Thus, in a proglacial environment such as Burfu, the optimum interpretation of oxygen isotope values would be a mass-balance approach between relative amounts of glacial meltwater and direct precipitation.

A mass-balance approach is also used for the interpretation of carbon isotopes. The $\delta^{13}\text{C}$ from the carbonate in the Burfu lake sediments depends on the $\delta^{13}\text{C}$ values of the dissolved inorganic carbon (DIC) of the lake water. Two major sources of DIC include oxidized organic carbon ($\sim -10\text{‰}$ to $\sim -30\text{‰}$) and dissolved marine carbonates ($\sim -2\text{‰}$ to $+2\text{‰}$) (Fritz and Fontes, 1980). The input of dissolved marine carbonates depends on the amount of chemical weathering in the catchment area, which depends on the exposed surface area of the catchment, the ambient temperature, and rainfall. Depleted $\delta^{13}\text{C}$ implies low input of carbonate and hence a combination of low weathering, low exposed surface and low rainfall. Given a catchment dominated by Tethyan carbonates, it is reasonable to assume that changes in climate would change chemical weathering rates and also the amount of dissolved carbonates that is delivered to the Burfu lake. Thus the Burfu $\delta^{13}\text{C}_{\text{carbonate}}$ values can be interpreted as a mass balance between oxidized organic carbon and dissolved carbonates as sources of DIC in the lake water.

Analogous to the discussion above, Jin et al. (2005) argued that the intensity of chemical weathering in the Tibetan Plateau depends on

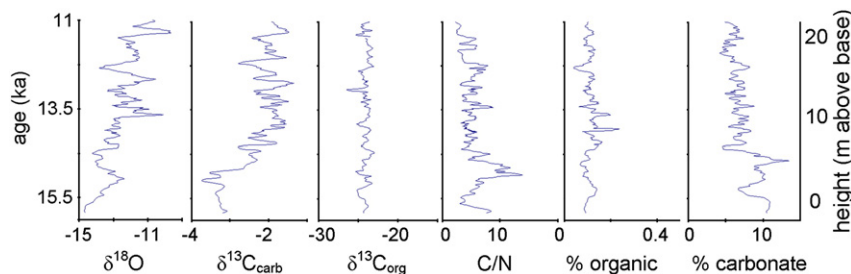


Figure 6. Isotope data from Burfu lacustrine sediments. Stable isotope values are given in standard ‰ notation with respect to VPDB.

temperature and monsoon intensity (both positively correlated), and thus it should respond to well-known global climatic events, such as the Younger Dryas and Holocene Optimum. In the Garhwal Himalaya, Barnard et al. (2004a,b) demonstrated that periods of enhanced monsoon resulted in major resedimentation events. Further, Jacobson et al. (2002) provided geochemistry data for streams in the Himalaya, indicating that they are dominated by Ca^{2+} – Mg^{2+} – HCO_3^- ions, with chemical weathering of carbonates contributing more dissolved ions than weathering of silicates (e.g., Sarin et al., 1989; Bartarya, 1993; Harris et al., 1998; Singh and Hasnain, 1998; Singh et al., 1998a; Galy and France-Lanord, 1999; Pandey et al., 1999; Dalai et al., 2002).

Table 3 gives the difference between calibrated radiocarbon dates of the carbonate fraction and OSL-model ages. We interpret the difference as a qualitative measure of the amount of DIC into the lake and hence the magnitude of chemical weathering of carbonates. It is also to be noted that any error on account of incomplete bleaching of the OSL signal would result in higher OSL ages (Aitken, 1985; Lian and Roberts, 2006). If poor bleaching were the case, the real age would be even younger, giving an even larger difference between OSL and radiocarbon ages. Thus the present comparison provides a conservative scenario of the hardwater effect in the present radiocarbon dates. The isotopic data offer some support for this interpretation. The sample collected at 3.55 m above the base is more isotopically depleted ($\delta^{13}\text{C}_{\text{carbonate}} = -3.64\%$) than the other samples that were carbon dated, suggesting a smaller hardwater effect. This sample also shows a much smaller difference (5028 yr) between the calibrated ^{14}C age and the OSL-model age than the other samples, also suggesting a smaller hardwater effect (Table 3). Further, a positive correlation between the C/N ratio and the ^{14}C age of carbonates also supports the above discussion (Fig. 7). Low C/N ratios indicate an aquatic origin for organic carbon, whereas C/N ratios >20 are typical of terrestrial organic matter (Meyers et al., 1984). Samples from this study with higher C/N ratios are also characterized by a larger hardwater effect. Higher terrestrial input would likely flush in a larger amount of dissolved Tethyan carbonates, and would thereby alter the ^{14}C age.

Climate variations

Unit-I: This unit of the Burfu lake begins with depleted oxygen isotope values (-15%). This, along with relatively coarse-grained sediment, suggests that the lake received its initial water from melting glaciers (Fig. 8). Pant et al. (2006) interpreted the local geomorphology to suggest that the Burfu lake formed following the retreat of a glacier after the last glacial maximum. $\delta^{13}\text{C}_{\text{carbonate}}$ is very depleted (-3.5%) at the bottom of the lake section, suggesting a minimal input of dissolved carbonates. Thus the analysis of Unit-I suggests that in the early stages of the Burfu lake, a relatively cool climate and weak monsoon with a low rate of chemical weathering existed in the region (Fig. 8). Between 16 ka and ~ 14.5 ka, the $\delta^{18}\text{O}$ values steadily increased from -15% to $\sim -13\%$, suggesting that a greater proportion of the source water was from direct precipitation on the lake, i.e. a strengthened monsoon.

At ~ 14.5 ka a sudden warming event occurred as indicated by an abrupt shift in $\delta^{13}\text{C}_{\text{carbonate}}$ from -3.5% to -2.5% (Fig. 8) and a decrease in oxygen isotope values. This suggests a large pulse of

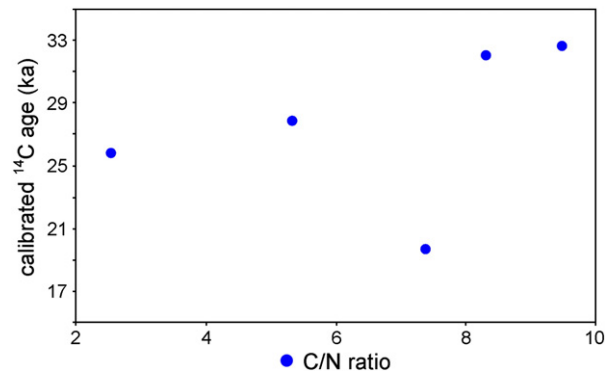


Figure 7. Plot of C/N ratio vs. calibrated $^{14}\text{C}_{\text{carbonate}}$ age (in calendar years).

glacial meltwater that fed the lake during this time. The retreat of glaciers provided an extended carbonate surface for weathering that led to the sudden enrichment of $\delta^{13}\text{C}_{\text{carbonate}}$ values due to a larger contribution of dissolved carbonates to the DIC of the lake. Thus the climate at this time was warmer with a strong monsoon. The overall timing of this is similar to the onset of the Bølling–Allerød and the Atlantic sea-level rise caused by Meltwater Pulse 1a, as documented in the Barbados coral sediments (Fairbanks, 1989).

During this time interval C/N ratios also increased to values near 15 (Fig. 8). In general, organic carbon in the Burfu section has a low C/N ratio characteristic of an aquatic signature. The exception is the time interval from ~ 14.5 to ~ 14.2 ka, during which a significant contribution from terrestrial sources is indicated. A greater contribution from terrestrial organic carbon is consistent with an increase in glacial meltwater and increased runoff due to increased temperature and monsoon precipitation (Sirocko et al., 1993).

Unit-II: This unit is characterized by an overall increasing trend in both $\delta^{18}\text{O}$ and $\delta^{13}\text{C}_{\text{carbonate}}$ (Fig. 8). Two ^{14}C dates from Unit-II samples show a significant hardwater effect. A greater hardwater effect and an increase in $\delta^{13}\text{C}_{\text{carbonate}}$ values together suggest an increased contribution of dissolved carbonates to the DIC of the lake water. The overall increasing trend in $\delta^{18}\text{O}$ implies a higher monsoon precipitation/glacial meltwater ratio for the source waters to the Burfu lake.

Superimposed on the increasing trends in isotope values are several high-amplitude changes in $\delta^{13}\text{C}_{\text{carbonate}}$ and $\delta^{18}\text{O}$ (Fig. 8). In this unit, sediments comprise clay varve/rhythmite layers with occasional dropstones. This is interpreted as an unstable climate, characterized by large changes in temperature, chemical weathering rates, and hydrologic inputs. Taken together, the data in Unit-II suggest an overall warming, unstable climate, and an intensification of the monsoon.

Unit-III: This unit is characterized by a sharp decrease in $\delta^{18}\text{O}$ and $\delta^{13}\text{C}_{\text{carbonate}}$ at ~ 12.5 ka. Low $\delta^{18}\text{O}$ values at the beginning of this unit imply a change in the balance of source waters for the Burfu lake, with a greater proportion derived from isotopically depleted sources (i.e., glacial meltwater) and with a reduced contribution from monsoon precipitation. The low value for $\delta^{13}\text{C}_{\text{carbonate}}$ indicates a decrease in the chemical weathering of carbonates, consistent with a weakened monsoon.

Following this brief (~ 300 -yr) cold interval, there is an increase of $\delta^{13}\text{C}_{\text{carbonate}}$ and $\delta^{18}\text{O}$ values to Unit-II levels, after which $\delta^{13}\text{C}_{\text{carbonate}}$ gradually decreases during ~ 12 to ~ 11.5 ka (Fig. 8). These data suggest that climate in North India during this period was intensely cool followed by a longer (~ 500 yr) period of moderate climate. It is interesting to note that this was also the time of the Younger Dryas cold excursion.

Although it is speculative to draw conclusions on time intervals that are smaller than the error range for the OSL dates, similar trends do exist in other proxy records. The oxygen isotope record from a

Table 3

Difference between calibrated radiocarbon ages of carbonate and corresponding OSL-model ages.

| Height (m above bottom) | Age (^{14}C yr BP) | Calibrated age (yr BP) | Model age (cal. ^{14}C age-model age) | Difference | $\delta^{13}\text{C}_{\text{carbonate}}$ |
|-------------------------|------------------------------|------------------------|--|------------|--|
| 19.05 | 21,440 \pm 150 | 25,741 \pm 243 | 11,200 | 14,541 | -1.57 |
| 15.35 | 26,720 \pm 260 | 32,007 \pm 317 | 12,014 | 19,993 | -2.30 |
| 13.85 | 23,180 \pm 200 | 27,811 \pm 264 | 12,324 | 15,487 | -2.11 |
| 11.2 | 27,300 \pm 280 | 32,625 \pm 335 | 12,916 | 19,709 | -2.02 |
| 3.55 | 16,524 \pm 87 | 19,638 \pm 107 | 14,610 | 5,028 | -3.64 |

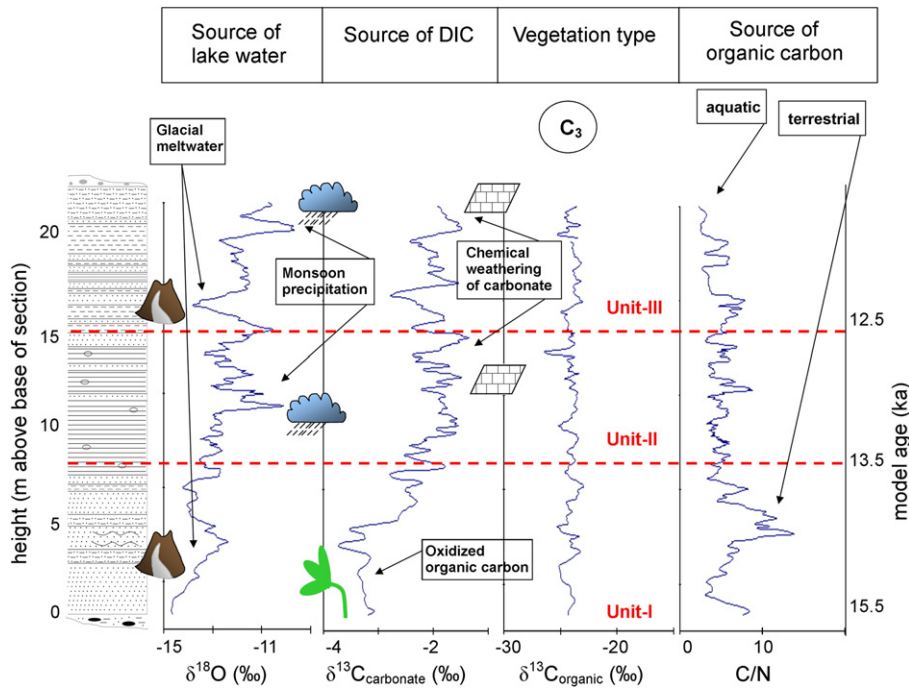


Figure 8. Conceptual diagram showing stable isotope ratios, C/N ratios, and generalized interpretations.

speleothem at Timta cave in North India also shows a shift in oxygen isotope values mid-way through the Younger Dryas (Sinha et al., 2005). Jin et al. (2005) presented evidence for a shorter Younger Dryas interval in Tibet than in the North Atlantic region. Juyal et al.'s (2004) data from a relict lake at Garbayang (in the Kali River basin adjoining Burfu) show a sudden drop in magnetic susceptibility and elemental concentration corresponding to the period between 11 and 12 ka that has been attributed to the Younger Dryas cooling event.

A warming at 11.3 ka in the Burfu section is indicated by an increase in both carbon and oxygen isotope values, suggesting an abrupt warming and intensification of the monsoon, resulting in an increase in the contribution of dissolved carbonates to the DIC of the lake water (Fig. 8). A calibrated ¹⁴C age of 25,740 ± 240 cal yr BP in these sediments shows an amplified hardwater effect, and thus supports an intensified monsoon and enhanced chemical weathering of carbonates.

Throughout the entire Burfu lacustrine section, δ¹³C values from the organic fraction are relatively constant at ~−23‰. In certain environments, δ¹³C from the organic fraction of lacustrine sediments can inform on past climates via changes in vegetation history (Krishnamurthy et al., 1986). A nearly constant δ¹³C from the Burfu lacustrine section indicates the dominance of C₃ vegetation with minor changes in the amount of C₄ vegetation (Fig. 8). The dominance of C₃ vegetation near Burfu throughout this time interval is consistent with results from organic material from loess deposits across China (Liu et al., 2005), which also show a dominance of C₃ vegetation during the late Pleistocene. Liu et al. (2005) observed evidence for an expansion of C₄ vegetation near the coast of China during the late Pleistocene. However, the expansion of C₄ vegetation was not observed in areas of lower average temperature and precipitation in the interior of the continent (Liu et al., 2005), i.e. environments similar to Burfu.

A similarity between the present data and the oxygen isotope data from a speleothem from Timta Cave (29°50'17"N, 80°02'01"E, 1900 m.a.s.l.) by Sinha et al. (2005) exists (Fig. 9). Oxygen isotopes from the Timta Cave study were interpreted as a proxy for the intensity of the monsoon, with the primary control on isotope fractionation being the 'amount effect', i.e. depleted δ¹⁸O resulting from an increase in monsoon precipitation. Both the Burfu and Timta

studies show a weak monsoon in North India at ~15.5 ka that increased until ~12.6 ka. High-amplitude variations are present in both studies during the time interval from ~13 ka to ~12.5 ka, and a sharp change in oxygen isotope values at ~12.7 ka to ~12.3 ka indicates a significant decrease in the intensity of the monsoon. Both studies interpret this significant isotope shift as the Younger Dryas. Discrepancies in timing and in isotopic changes may be related to i) dating errors, and ii) differences in localized factors that may affect isotope fractionation, i.e. Burfu in a proglacial environment and Timta in the influence of the vadose zone.

Conclusions

Lacustrine sediments near Burfu in the Goriganga valley are broadly dated by OSL from ~16 ka to ~11 ka. The results presented here appear to suggest correlations to global climate events, given the error margins associated with the OSL dates. Radiocarbon ages are not used in the age model because of a pronounced hardwater effect but are used to provide a qualitative estimate of the magnitude of hardwater-induced contamination, which is proportional to the chemical weathering of carbonates. We interpret the δ¹⁸O as a mass balance between depleted glacial meltwater and more enriched

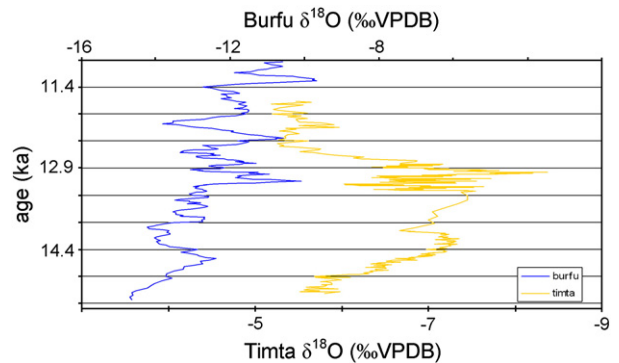


Figure 9. Oxygen isotope values from Burfu lake sediments (blue line on left) and Timta Cave speleothem (yellow line on right) (Sinha et al., 2005).

monsoon precipitation as sources for the lake water, and we interpret $\delta^{13}\text{C}_{\text{carbonate}}$ as a mass balance between isotopically depleted oxidized organic carbon and isotopically enriched dissolved carbonate as sources of DIC in the lake water.

The oxygen and carbon isotope data are depleted at the bottom of the section, suggesting a cool glacial climate, with an abrupt increase occurring at ~14.5 ka, which may correlate with the North Atlantic Meltwater Pulse 1a. The middle section, from ~13.2 ka to ~12.5 ka, is characterized by more enriched values of oxygen and carbon isotopes with high-amplitude oscillations in isotope values. This time period may correlate with the Bølling–Allerød. The data suggest a strong monsoon and a high rate of chemical weathering with periods of climatic instability. At ~12.5 ka a sharp decrease in oxygen and carbon isotope values signifies a weak monsoon, possibly coincident with the Younger Dryas. Following this, at ~11.3 ka there is a sudden shift in the isotope data toward more enriched values, interpreted as an abrupt increase in monsoon intensity and the magnitude of chemical weathering of carbonates.

Acknowledgments

Funding for the stable isotopic and radiocarbon analysis of the project was provided by the Michigan Space Grant Consortium. AMS ^{14}C dates were performed at the NSF University of Arizona AMS facility. OSL dates were measured at the Physical Research Laboratory, India. N. Juyal and N. Basavaiah collected the samples and documented the geomorphology and geology along with Dr. R.K. Pant. We thank Associate Editor Dr. L. Owen and two reviewers for their patience and constructive suggestions.

References

Aitken, M.J., 1985. Thermoluminescence Dating. Academic Press, London.

Barnard, P.L., Owen, L.A., Finkel, R.C., 2004a. Style and timing of glacial and paraglacial sedimentation in a monsoon-influenced high Himalayan environment, the upper Bhagirathi Valley, Garhwal Himalaya. *Sedimentary Geology* 165 (3), 199–221.

Barnard, P.L., Owen, L.A., Sharma, M.C., Finkel, R.C., 2004b. Late Quaternary (Holocene) landscape evolution of a monsoon-influenced high Himalayan valley, Gori Ganga, Nanda Devi, NE Garhwal. *Geomorphology* 61, 91–110.

Bartarya, S.K., 1993. Hydrochemistry and rock weathering in a subtropical Lesser Himalayan river basin in Kumaun. *Journal of Hydrology* 146, 149–174.

Bush, A.B.G., 2000. A positive climatic feedback mechanism for Himalayan glaciation. *Quaternary International* 65 (66), 3–13.

Chandel, H.N., Patel, A.D., Vaghela, H.R., Ubale, G.P., 2006. An effective and reuseable sampling pipe for luminescence dating. *Ancient TL* 24 (1), 21–22.

Dalai, T.K., Krishnaswami, S., Sarin, M.M., 2002. Major ion chemistry in the headwaters of the Yamuna river system: chemical weathering, its temperature dependence and CO_2 consumption in the Himalaya. *Geochimica et Cosmochimica Acta* 66 (19), 3397–3416.

Fairbanks, R.G., 1989. A 17,000-year glacio-eustatic sea level record: influence of glacial melting rates on the Younger Dryas event and deep-ocean circulation. *Nature* 342, 637–642.

Fairbanks, R.G., Mortlock, R.A., Chiu, T.-C., Cao, L., Kaplin, A., Guilderson, T.P., Fairbanks, T.W., Bloom, A.L., 2005. Marine radiocarbon calibration curve spanning 0 to 50,000 years B.P. based on paired $^{230}\text{Th}/^{234}\text{U}$ and ^{14}C dates on pristine corals. *Quaternary Science Reviews* 24, 1781–1796.

Fontes, J.-C., Gasse, F., Gibert, E., 1996. Holocene environmental changes in Bangong Co Basin (Western Tibet): Part 1. Chronology and stable isotopes of carbonates of a Holocene lacustrine core. *Palaeogeography, Palaeoclimatology, Palaeoecology* 120, 25–47.

Fritz, P., Fontes, J.C. (Eds.), 1980. Handbook of environmental isotope geochemistry. Volume 1: the terrestrial environment. Elsevier, Amsterdam.

Fuchs, M., Owen, L.A., 2008. Luminescence dating of glacial and associated sediments: review, recommendations and future directions. *Boreas* 37, 636–659.

Galy, A., France-Lanord, C., 1999. Weathering processes in the Ganges-Brahmaputra basin and the riverine alkalinity budget. *Chemical Geology* 159, 31–60.

Ghosh, P., Bhattacharya, S.K., 2003. Sudden warming epochs during 42 to 28 ky B.P. in the Himalayan region from stable isotope record of sediment column from a relict lake in Goting, Garhwal, North India. *Current Science* 85 (1), 60–67.

Harris, N., Bickle, M., Chapman, H., Fairchild, I., Bunbury, J., 1998. The significance of Himalayan rivers for silicate weathering rates: evidence from the Bhote Kosi tributary. *Chemical Geology* 144, 205–220.

Jacobson, A.D., Blum, J.D., Walter, L.M., 2002. Reconciling the elemental and Sr isotope composition of Himalayan weathering fluxes: insights from the carbonate geochemistry of stream waters. *Geochimica et Cosmochimica Acta* 66 (19), 3417–3429.

Jin, Z.-D., Wu, Y., Zhang, X., Wang, S., 2005. Role of late glacial to mid-Holocene climate in catchment weathering in the central Tibetan Plateau. *Quaternary Research* 63, 161–170.

Juyal, N., Pant, R.K., Basavaiah, N., Yadava, M.G., Saini, N.K., Singhvi, A.K., 2004. Climate and seismicity in the higher Central Himalaya during 20–10 ka: evidence from the Garbayang basin, Uttarakhand, India. *Palaeogeography, Palaeoclimatology, Palaeoecology* 213, 315–330.

Juyal, N., Chamyal, L.S., Bhandari, S., Bhushan, R., Singhvi, A.K., 2006. Continental record of the southwest monsoon during the last 130 ka: evidence from the southern margin of the Thar Desert, India. *Quaternary Science Reviews* 25, 2632–2650.

Krishnamurthy, R.V., Bhattacharya, S.K., Kusumgar, S., 1986. Palaeoclimatic changes deduced from $^{13}\text{C}/^{12}\text{C}$ and C/N ratios of Karewa lake sediments, India. *Nature* 323, 150–152.

Krishnamurthy, R.V., Atekwana, E.A., Guha, H., 1997. A simple, inexpensive carbonate-phosphoric acid reaction method for the analysis of carbon and oxygen isotopes of carbonates. *Analytical Chemistry* 69 (20), 4256–4258.

Krishnamurthy, R.V., Syrup, K., Long, A., 1999. Is selective preservation of nitrogenous organic matter reflected in the d^{13}C signal of lacustrine sediments? *Chemical Geology* 158, 165–172.

Kronborg, C., 1983. Preliminary results of age determination by TL of interglacial and interstadial sediments. *PACT* 9, 595–605.

Leng, M.J., Marshall, J.D., 2004. Palaeoclimate interpretation of stable isotope data from lake sediment archives. *Quaternary Science Reviews* 23, 811–831.

Lian, O.B., Roberts, R.G., 2006. Dating the quaternary: progress in luminescence dating of sediments. *Quaternary Science Reviews* 25, 2449–2468.

Liu, W., Huang, Y., An, Z., Clemens, S., Li, L., Prell, W., Ning, Y., 2005. Summer monsoon intensity controls C_4/C_3 plant abundance during the last 35 ka in the Chinese Loess Plateau: carbon isotope evidence from bulk organic matter and individual leaf waxes. *Palaeogeography, Palaeoclimatology, Palaeoecology* 220, 243–254.

Meyers, P.A., Leenheer, M.J., Eadie, B.J., Maule, S.J., 1984. Organic geochemistry of suspended and settling particulate matter in Lake Michigan. *Geochimica et Cosmochimica Acta* 48, 443–452.

Murray, A.S., Wintle, A.G., 2000. Luminescence dating of quartz using an improved single aliquot regenerative dose protocol. *Radiation Measurements* 32, 57–73.

Owen, L.A., Sharma, M.C., 1998. Rates and magnitudes of paraglacial fan formation in the Garhwal Himalaya: implications for landscape evolution. *Geomorphology* 26, 171–184.

Pandey, S.K., Singh, A.K., Hasnain, S.I., 1999. Weathering and geochemical processes Controlling solute acquisition in Ganga Headwater-Bhagirathi River, Garhwal Himalaya, India. *Aquatic Geochemistry* 5, 357–379.

Pant, R.K., Juyal, N., Basavaiah, N., Singhvi, A.K., 2006. Late Quaternary glaciation and seismicity in the Higher Central Himalaya: evidence from Shalng basin (Goriganga), Uttarakhand. *Current Science* 90 (11), 1500–1505.

Prell, W.L., Kutzbach, J.E., 1992. Sensitivity of the Indian monsoon to forcing parameters and implications for its evolution. *Nature* 360, 647–652.

Sarin, M.M., Krishnaswami, S., Dilli, K., Somayajulu, B.L.K., Moore, W.S., 1989. Major ion chemistry of the Ganga-Brahmaputra River system: weathering processes and fluxes to the Bay of Bengal. *Geochimica et Cosmochimica Acta* 53, 997–1009.

Sharma, M.C., Owen, L.A., 1996. Quaternary glacial history of the Garhwal Himalaya, India. *Quaternary Science Reviews* 15, 335–365.

Singh, A.K., Hasnain, S.I., 1998. Major ion chemistry and weathering control in a high altitude basin: Alaknanda River, Garhwal Himalaya, India. *Hydrological Sciences Journal* 43, 825–843.

Singh, A.K., Pandey, S.K., Panda, S., 1998. Dissolved and sediment load characteristics of Kafni Glacier meltwater, Pindar Valley, Kumaon Himalaya. *Journal of the Geological Society of India* 52, 305–312.

Singhvi, A.K., Bluszcz, A., Bateman, M.D., Rao, S., 2001. Luminescence dating of loess-paleosol sequences coversands: methodological aspects and paleoclimatic implications. *Earth Science Reviews* 54, 193–211.

Singhvi, A.K., Porat, N., Wagner, G.A., Eitel, B., 2011. Luminescence dating in earth sciences. In: Krbetschek, M., et al. (Ed.), *Handbook of Luminescence Dating*. Springer Verlag, Heidelberg.

Sinha, A., 1981. Geology and tectonics of the Himalayan region of Ladakh, Himanchal, Garhwal-Kumaun and Arunachal Pradesh: a review. *Zagros, Hindukush, Himalaya geodynamic evolution, Geodynamics series. Am. Geophys. Union* 3, 122–148.

Sinha, A., Cannariato, K.G., Stott, L.D., Li, H.-C., You, C.-F., Cheng, H., Edwards, R.L., Singh, I.B., 2005. Variability of Southwest Indian summer monsoon precipitation during the Bølling–Allerød. *Geology* 33 (10), 813–816.

Sirocko, F., Sarnthein, M., Erlenkeuser, H., Lange, H., Arnold, M., Duplessy, J.C., 1993. Century-scale events in monsoonal climate over the past 24,000 years. *Nature* 364, 322–324.